

8-Alkoxy- and 8-AryloxyBODIPYs: Straightforward Fluorescent Tagging of Alcohols and Phenols.

Juan O. Flores-Rizo, Ixone Esnal, Carlos A Osorio-Martínez, Cesar Fernando A Gomez-Duran, Jorge Bañuelos, Iñigo Lopez Arbeloa, Keith H. Pannell, Alejandro J. Metta-Magana, and Eduardo Peña-Cabrera

J. Org. Chem., **Just Accepted Manuscript** • DOI: 10.1021/jo400417h • Publication Date (Web): 30 May 2013

Downloaded from <http://pubs.acs.org> on June 2, 2013

Just Accepted

"Just Accepted" manuscripts have been peer-reviewed and accepted for publication. They are posted online prior to technical editing, formatting for publication and author proofing. The American Chemical Society provides "Just Accepted" as a free service to the research community to expedite the dissemination of scientific material as soon as possible after acceptance. "Just Accepted" manuscripts appear in full in PDF format accompanied by an HTML abstract. "Just Accepted" manuscripts have been fully peer reviewed, but should not be considered the official version of record. They are accessible to all readers and citable by the Digital Object Identifier (DOI®). "Just Accepted" is an optional service offered to authors. Therefore, the "Just Accepted" Web site may not include all articles that will be published in the journal. After a manuscript is technically edited and formatted, it will be removed from the "Just Accepted" Web site and published as an ASAP article. Note that technical editing may introduce minor changes to the manuscript text and/or graphics which could affect content, and all legal disclaimers and ethical guidelines that apply to the journal pertain. ACS cannot be held responsible for errors or consequences arising from the use of information contained in these "Just Accepted" manuscripts.

8-Alkoxy- and 8-AryloxyBODIPYs: Straightforward Fluorescent Tagging of Alcohols and Phenols.

Juan O. Flores-Rizo,[£] Ixone Esnal,[†] Carlos A. Osorio-Martínez,[£] César F. A. Gómez-Durán,[£] Jorge Bañuelos,[†] Iñigo López Arbeloa,^{*,†} Keith H. Pannell,[‡] Alejandro J. Metta-Magaña,[‡] and Eduardo Peña-Cabrera.^{*,£}

[£] Departamento de Química, Universidad de Guanajuato. Col. Noria Alta S/N. Guanajuato, Gto. 36050, Mexico,

[†] Departamento de Química Física. Universidad del País Vasco/EHU. Aptdo 644, 48080, Bilbao, Spain

[‡] Department of Chemistry. The University of Texas at El Paso. 500 W. University Ave., El Paso, TX 79968. USA.

inigo.lopezarbeloa@ehu.es, eduardop@ugto.mx

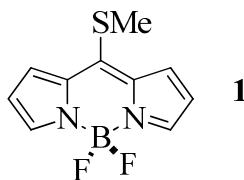
ABSTRACT

We demonstrate herein that both alcohols and phenols can be tagged with a BODIPY (borondipyrromethene) moiety to yield highly fluorescent products. Thus, 8-(methylthio)BODIPY **1** undergoes S_NAr-type reaction with a host of alcohols and phenols in the presence of a base and a Cu(I) additive. The BODIPY dyes bearing alkoxy or non-functionalized phenoxy moieties are characterized by a highly efficient fluorescence emission, regardless of the media, in the blue-green part of the visible. Complementary, the presence of electron donor groups at the aryl ring leads to an intramolecular charge transfer process, which quenches the fluorescence mainly in polar media. In addition to simple alcohols and phenols, four natural products (eugenol, menthol, cholesterol and estrone) were labeled in a simple fashion. X-ray structures of the cholesterol and estrone derivatives were discussed. In fact, the BODIPY bearing cholesterol stands out as a bright fluorescence biological marker.

Introduction

Applications seemingly unrelated such as the design of drug nanocarriers used in theranostics (area of research that combines diagnostic detection agents with therapeutic drug delivery carriers)¹ and recently reported conjugated materials used in solution-processed solar cells² have one thing in common: they both contain one or several BODIPY (borondipyrromethene) units. Among their most useful properties are: Strong absorbance in the visible wavelengths, narrow absorption bands, and tunable photophysics that can allow one vary both the quantum yield (Φ_F) and emission wavelength (λ_{em}).⁴ This type of dyes has found ample use in biology⁵ and materials science⁶ due to the fact that they can be grafted onto the substrate of interest, thereby making it fluorescent, or fluorescent-prone.

After the seminal report by Biellmann *et al.* in 2006, which described the synthesis and optical properties of 8-(methylthio)BODIPY **1**,⁷ our research groups have demonstrated that such compound can efficiently participate in a variety of useful chemical transformations.



For example, **1** participates in the Liebeskind-Srogl cross-coupling reaction⁸ with boronic acids to yield the corresponding 8-substituted BODIPY derivatives.⁹ Also, the methylthio group can be replaced by a proton to produce the parent unsubstituted BODIPY system in almost quantitative yield.¹⁰ We have shown as well that the methylthio group could be substituted by primary and secondary amines to give highly fluorescent blue-emitting analogues, a property hitherto unknown for BODIPY dyes.¹¹ In this way, blue emitting BODIPYs were developed with improving fluorescence and lasing performance with regard to commercially available laser dyes in that region. The reason of such unexpected behavior was that the BODIPY delocalized π -system, characterized as a cyclic cyanine, changes to a hemicyanine-like one upon the presence of the amino group. However, the fluorescence efficiency of the derivatives

bearing secondary and tertiary amines was limited in polar media by the activation of a quenching intramolecular charge transfer (ICT) process.

Although BODIPY dyes have been conjugated to many biologically relevant molecules,¹² a big synthetic effort has to be devoted to the modification of the BODIPY core in order to add a functional group that would allow the attachment to the target molecule under mild conditions. Alternatively, one can purchase the commercially available dyes³ already functionalized for the desired purposes, albeit at sky-high prices.

On the other hand, intriguing research possibilities arise given the opportunity to tag hydroxylated complex molecules (i.e., molecules in Chart 1) with a fluorescent moiety under mild reaction conditions.

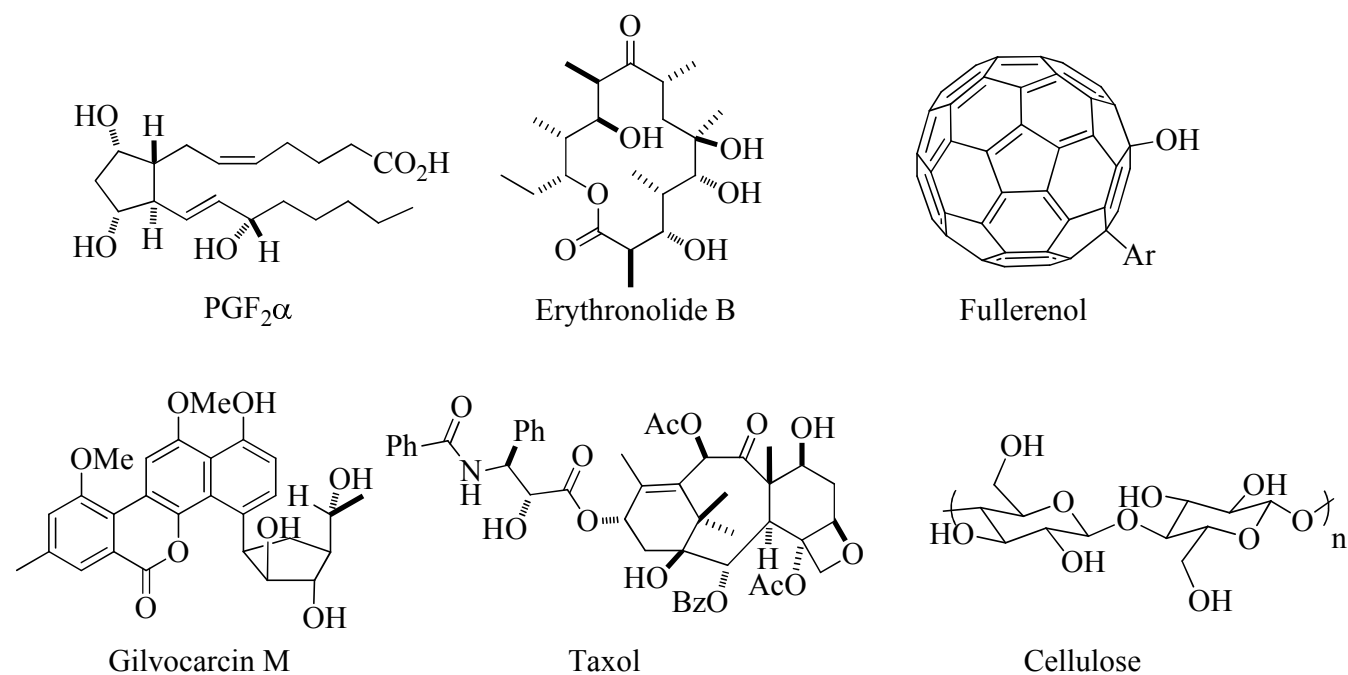
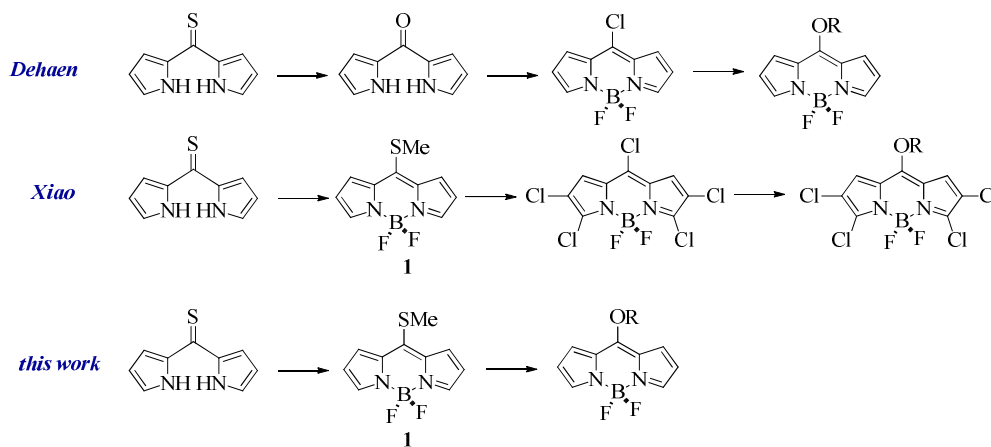


Chart 1. Hydroxylated complex products

The mode of action of important drugs may be elucidated using highly sensitive fluorescent techniques. The fabrication of fluorescent new materials, with potentially very useful properties may become a reality. In this context, we wish to disclose our efforts to *directly* attach alcohols and phenols to the BODIPY core via de displacement of the methylthio group to yield highly fluorescent dyes. Recently, both Dehaen and Xiao have reported the properties of a few examples of similar compounds by means of somewhat longer routes (Scheme 1).¹³

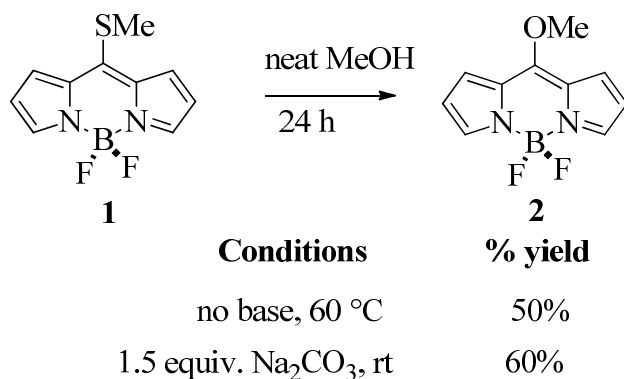


Scheme 1. Different ways to prepare alkoxyBODIPYs

Herein, we have carried out a more comprehensive study of this family of compounds. In addition to demonstrating the synthetic utility of this methodology, we have introduced alkoxy and aryloxy groups in the *meso* BODIPY position with the aim to modulate the extension of the blue-shift looking for tailor-made BODIPYs in an almost unexploited region with this fluorophore. Contrary to the fluorescence behavior of the aminoBODIPYs in polar solvents, 8-alkoxyBODIPYs developed herein excel by its bright green fluorescence, regardless of the media.

Results and Discussion

Synthesis. Prompted by our reports of the mild S_NAr -like displacement of the methylthio group in **1** with amines,¹¹ we set out to investigate similar displacement reaction with alcohols and phenols. In the initial trials, the desired product was obtained in 50% yield simply by stirring **1** in neat MeOH at 60 °C for 24 h. A slight yield increase (60%) was observed after 24 h at rt if 1.5 equiv. of Na_2CO_3 was added (Scheme 2).



Scheme 2. Initial reactions of **1** with neat MeOH

Realizing that these results were useful only for simple alcohols, we decided to investigate a more general and efficient way to carry out the same transformation using stoichiometric amounts of the reactants. The transformation of a thiol ester into an ester has been reported in the literature.¹⁴ This process is mediated by soft metal cations: Hg(II), Cu(I), Cu(II), and Ag(I). Coordination of the metal cation with the sulfur atom in the thiol ester weakens the S-C bond thereby facilitating the attack of the incoming alcohol. We hypothesized that a similar reactivity might be displayed by **1** drawing the analogy with thiol esters (Figure 1).

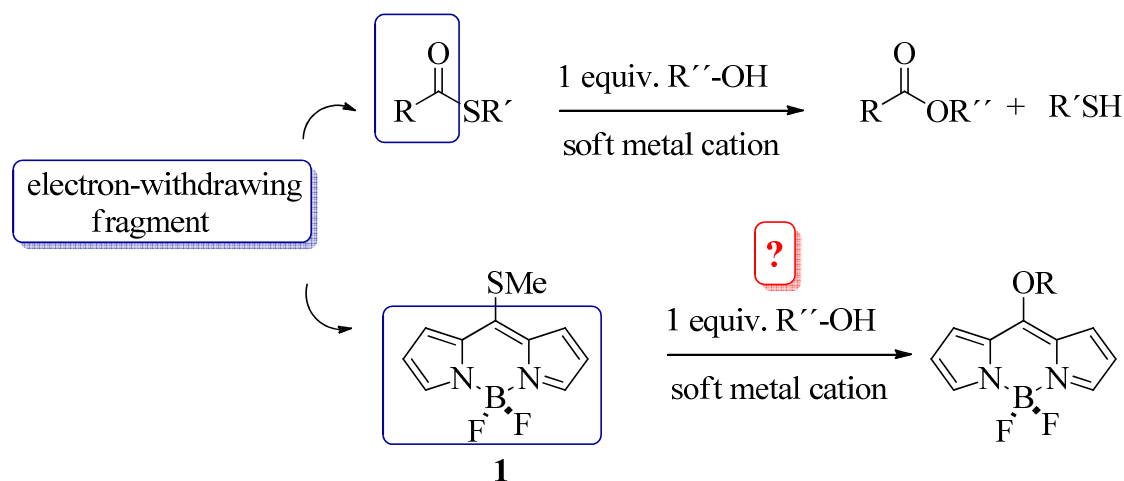
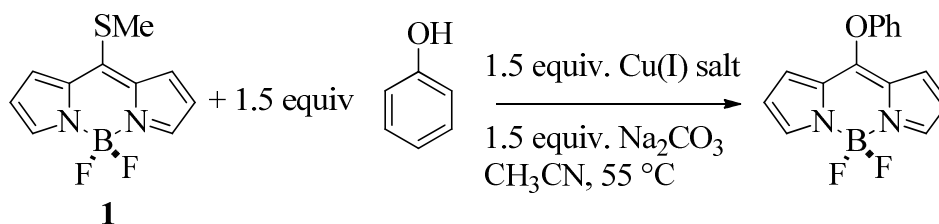


Figure 1. Analogy of the electronic properties of a thiol ester and those of **1**.

Since Cu(I) salts were considered to have the right combination of both low toxicity and cost, as compared to other soft metal cations such as Hg(II), a survey of the reactivity of different Cu(I) salts was undertaken (Table 1).

Table 1. Survey of Cu(I) salts on the formation of 8-alkoxyBODIPY dyes.

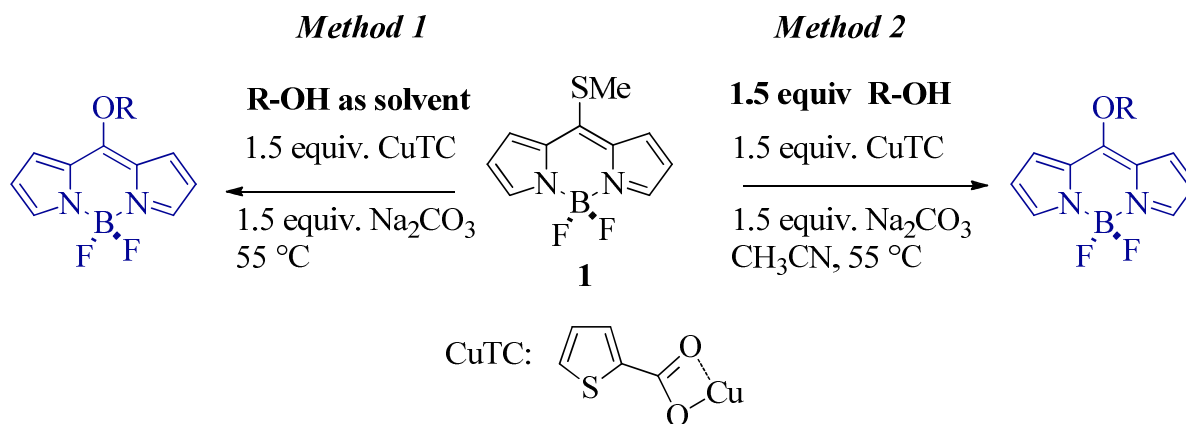
Entry	Cu(I) salt	% Conversion after 1h ^a
1	none	0
2	CuCl	34
3	CuCN	9
4	CuI	36
5	Cu(I)-3- Methylsalicylate	67
6	CuI-SMe ₂	31
7	Cu(I)OP(O)Ph ₂	47
8	Cu(I)OTf	21
9	CuTC ^b	100 ^c

^a Determined by ¹H NMR.^b Copper(I)- Thiophene-2-carboxylate.^c 90% isolated yield

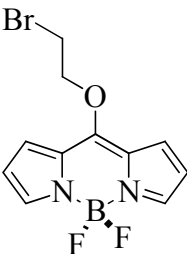
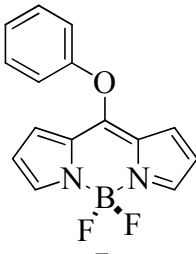
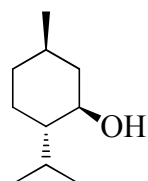
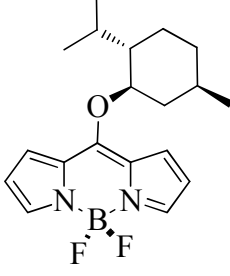
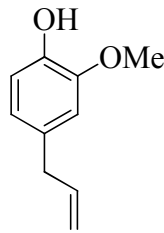
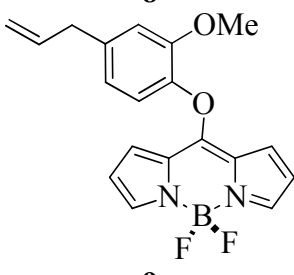
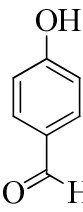
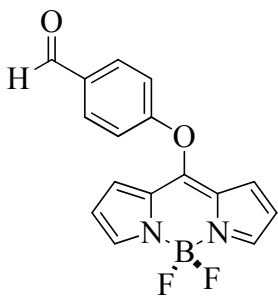
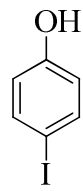
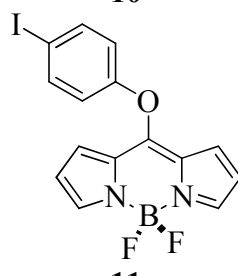
Although the majority of the Cu(I) salts showed some degree of activity, it was clear that copper(I)-thiophene-2-carboxylate (CuTC) was the most effective Cu(I) source since the desired product was obtained in 90% isolated yield with a complete conversion in under 1 h. Although no mechanistic study was undertaken, it might be argued that the driving force for the CuTC-mediated reaction is the formation of a strong S-CuTC bond (45-55 Kcal/mol) thereby labilizing further the C-S bond.¹⁵ The presence of a Cu(I) salt was essential as demonstrated by the control experiment shown in Entry 1. After the best reaction conditions were identified (CuTC, Na₂CO₃, CH₃CN), the generality of the process was

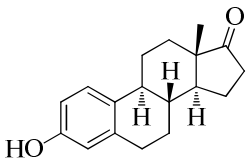
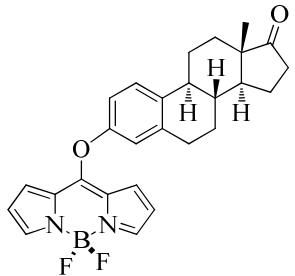
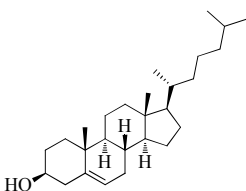
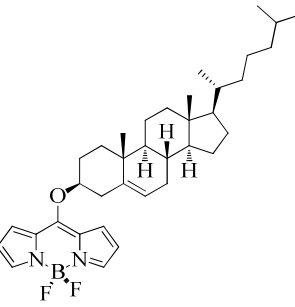
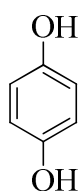
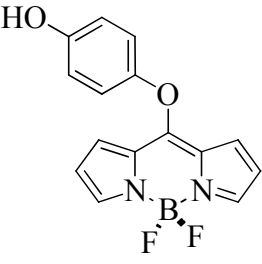
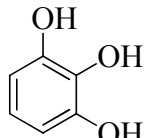
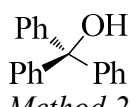
investigated with a series of both alcohols and phenols (Table 2). In Method 1, simple alcohols were used both as solvents and reactants, while in Method 2, the alcohol or phenol was used in slight excess in CH₃CN.

Table 2. Scope and limitations of the reaction of alcohols and phenols with **1**.



Entry	R-OH/Method	Compound	Reaction time (h)	% Yield ^a
1	MeOH <i>Method 1</i>	 2	1	73
2	EtOH <i>Method 1</i>	 3	3	62
3	Pr-OH <i>Method 1</i>	 4	4	70
4	<i>i</i> Pr-OH <i>Method 1</i>	-	-	-
5	Bu-OH <i>Method 2</i>	 5	3	67

6	Br-CH ₂ -CH ₂ -OH Method 2		6	66
7	PhOH Method 2		0.9	90
8	 Method 2		24	53
9	 Method 2		12	52
10	 Method 2		12	41
11	 Method 2		5	57

12	 <i>Method 2</i>	 12	5	76
13	 <i>Method 2</i>	 13	36	60
14	 <i>Method 2</i>	 14	2.5	56
15	 <i>Method 2</i>	-	-	-
16	 <i>Method 2</i>	-	-	-

^a Isolated yields

Using Method 1, simple alcohols added to **1** after only a few hours (Entries 1-3) to yield the corresponding 8-alkoxy dyes in acceptable yields. However, for reasons at this point unclear to us, *i*-PrOH failed to give the desired product for only decomposition was observed (Entry 4). Using Method 2, aliphatic alcohols displaced the methylthio group of **1** in moderate yields (Entries 5, 6, 8, 13). This reaction appears to be sensitive to steric effects; primary alcohols added within 3-6 h, while menthol and cholesterol added only after 24 and 36 h, respectively. Triphenylcarbinol failed to give the product altogether (Entry 15).

Phenols with different substitution patterns were added to **1** (Entries 7, 9, 10, 11, 12, 14). Phenol was the most reactive nucleophile since it efficiently added to **1** in 90% yield in less than 1 h (Entry 7). Addition of either electron-withdrawing or electron-donating substituents resulted in longer reaction times and moderate yields, with no discernible apparent pattern, at least in the sample of examples examined. As in the aliphatic alcohol series, steric crowding had a deleterious effect, pyrogallol also failed to add (Entry 15).

It is worth mentioning the functional group tolerance of particularly Method 2. As can be hinted from the examples presented herein, the potential of this method for numerous applications becomes clear. For instance, complex natural hydroxylated products (Entries 8, 9, 12 and 13) can be rendered fluorescent in one step via a very simple reaction. Similarly, some of the products prepared in this work contain functional groups that can be used as connecting points with other target molecules, or that can be interconverted to other for a specific application. For example, the bromine atom in **6**, the allyl group in **9**, the formyl group in **10**, the *p*-iodo atom in **11**, the carbonyl group in **12**, and the *p*-OH group in **14**.

Optical properties. With the results previously reported by us¹¹ for the 8-aminoBODIPY dyes as background, the properties of the new alkoxy and phenoxy derivatives are better understood. Figure 2 shows that both the absorption and fluorescence spectra of the methoxy derivative **2** are blue shifted with regard to the parent BODIPY chromophore, but to a lesser extent than the corresponding methylamino counterpart. Thus, while the amino substitution placed the absorption and emission bands at 418 nm and 463 nm, respectively, the alkoxy did it at 452 nm and 487 nm, enlarging the Stokes shift, in relation to the parent BODIPY (Figure 2). Theoretical calculations confirm this tendency. In general, the inclusion of electron donor substituents at the central position, characterized by a high enhancement of the electronic density upon excitation, increased the LUMO energy, whereas the HOMO orbital remained almost unaltered (Figure 3). Such increase of the energy gap depends on the electron-releasing ability of the substituent. Thus, the methoxy (Hammett parameter $\sigma_p = -0.268$) has a lower electron donor character in comparison with the methylamino ($\sigma_p = -0.84$) and consequently, the increase of the energy

gap is lower with the former substituent. Reported electrochemical measurements for a similar 8-methoxyBODIPY pointed out that the dye was more difficult to reduce, while the oxidation half-wave potential remained almost unaltered, confirming the above cited increase of the LUMO energy as the reason of the spectral blue-shift.^{13b}

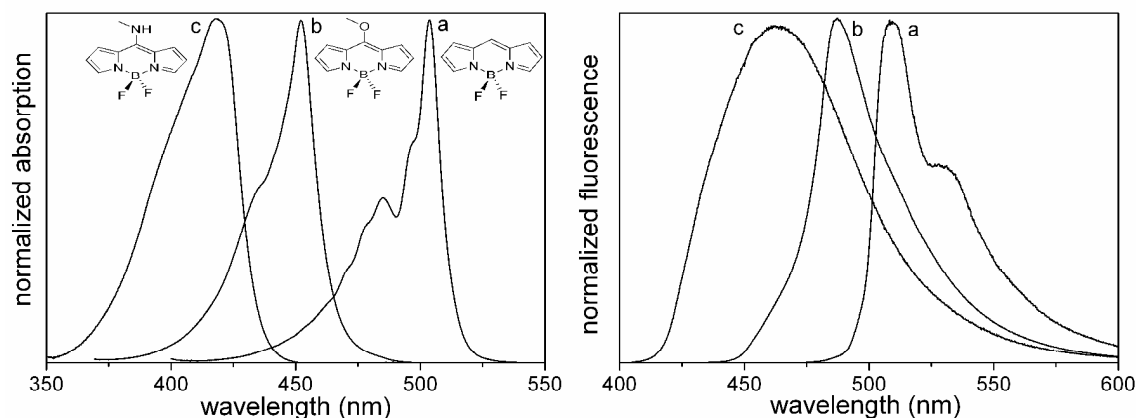


Figure 2. Normalized absorption and fluorescence spectra of BODIPY (a) and its methoxy (b) and methylamino (c) derivatives at central *meso* position in cyclohexane.

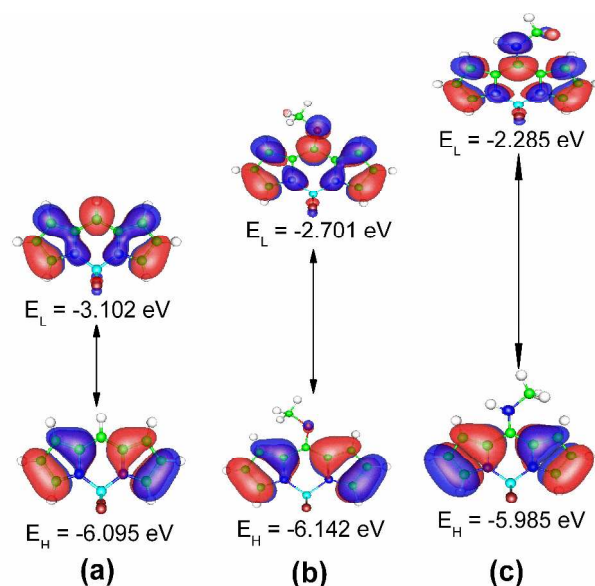


Figure 3. HOMO and LUMO eigenvalues for the parent BODIPY (a), and its derivatives bearing methoxy (b), and methylamino (c) at the central position.

The hypsochromic shift induced by the presence of heteroatoms at the *meso* position, is due to an important rearrangement of the electronic delocalization of the chromophore. The formation of a hemicyanine-like delocalized π -system due to the electron coupling of the amine and the BODIPY core (Figure 4), explains the shift induced by the amino group.¹¹ According to this argument, a methoxy group should also be able to interact by resonance with the chromophore, and hence, enable the formation of a merocyanine-like delocalization. The optimized ground state geometry places the oxygen coplanar with the chromophore, making possible the required electron coupling favoring the new resonant structure. The formation of these hemi and merocyanine delocalized π -systems from the cyanine one, upon grafting amino or methoxy, should imply an important charge rearrangement since both pyrroles are not longer equivalent. Accordingly, the shape of the spectral bands is altered (mainly in absorption where these resonant structures prevail) and they become broader and with lower vibrational resolution (Fig. 2). This feature is more evident with the amino group since the induced change in the chromophoric charge density by its higher electron releasing ability is stronger (Figure 4).

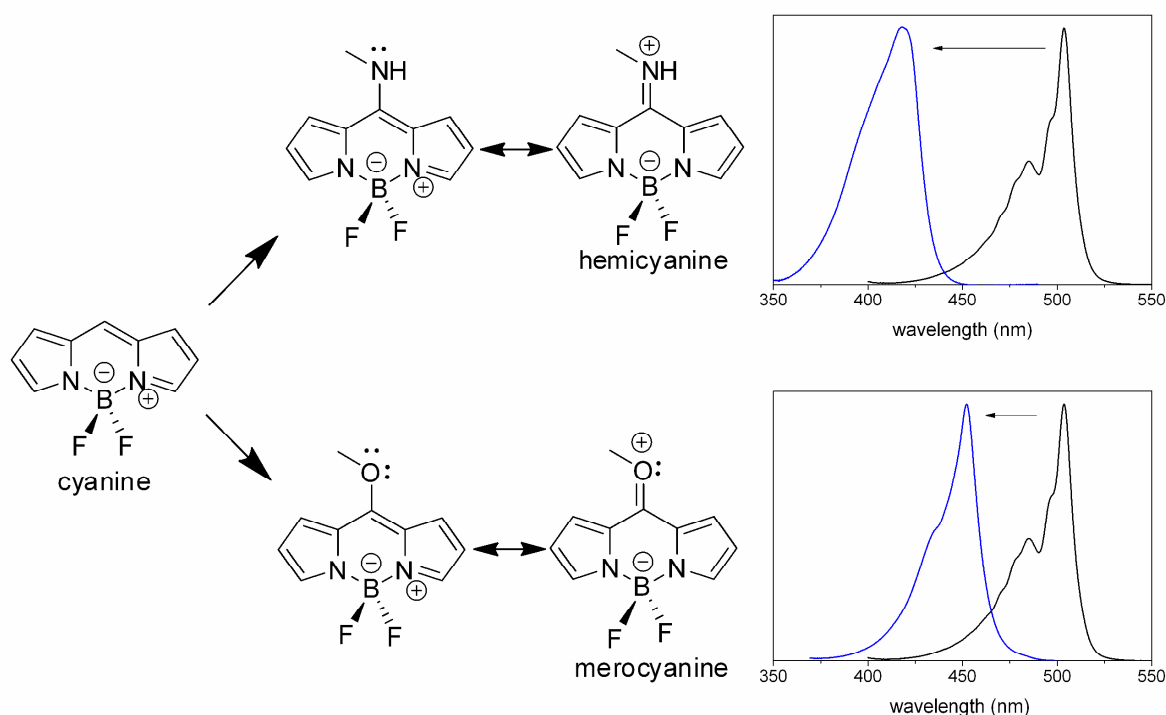


Figure 4. Hemicyanine and merocyanine resonant structures from a cyanine delocalized π -system upon the incorporation of heteroatoms (nitrogen and oxygen, respectively), at the central position of the BODIPY. The corresponding spectral hypsochromic shift of each new resonant structure is also plotted.

The fluorescence quantum yield of the BODIPY **2** is very high (around 0.8), regardless of the surrounding environment. At this point, it is important to note that the primary amino derivatives were highly fluorescent; however, secondary and tertiary amines caused a decrease of the fluorescence capacity in polar solvents because of activation of a quenching ICT state. Taking into account that the formation of such state depends directly on the electron releasing ability of the donor unit, the population of the ICT state should be hampered by the replacement of the methylamino group by the methoxy fragment. In fact, the high fluorescence efficiencies of dye **2** in all the considered solvents (Table 3), indicates that the ICT state is not taking place. This is a very important advantage since 8-methoxyBODIPY overcomes the limited fluorescence emission of 8-aminoBODIPYs in polar solvents.

Table 3. Photophysical properties of the parent unsubstituted BODIPY and its derivatives bearing alkoxy groups in a common apolar solvent (cyclohexane). The corresponding photophysical properties of 8-methylaminoBODIPY (8-MAB) have been included.^{11b} The data in a polar solvent (methanol) for methoxy and methylamino derivatives are also collected. The complete photophysical data in several solvents are included in Table 1S in SI.

	λ_{ab} (nm)	ϵ_{max} ($10^4 \text{ M}^{-1}\text{cm}^{-1}$)	λ_{fl} (nm)	ϕ	τ (ns)	k_{fl} (10^8 s^{-1})	k_{nr} (10^8 s^{-1})
BODIPY	503.5	7.6	510.5	0.96	6.47	1.48	0.06
2 (c-hexane)	452.0	6.0	487.0	0.84	5.41	1.55	0.29
2 (methanol)	441.0	4.6	485.5	0.75	6.14	1.22	0.41
8-MAB (c-hexane)	418.5	2.4	463.0	0.70	4.67	1.50	0.64

8-MAB	394.5	3.0	440.0	0.10	0.52	1.91	17.2
(methanol)							
3	451.0	6.2	486.5	0.96	5.44	1.76	0.07
4	450.5	6.4	486.0	0.93	5.43	1.71	0.13
5	450.0	6.0	486.0	0.80	5.43	1.47	0.37
13	451.5	5.3	485.0	0.91	5.58	1.63	0.16
8	450.5	6.2	486.0	0.88	5.63	1.56	0.21
6	455.5	4.5	491.0	0.91	5.57	1.63	0.16

Neither the length of the alkyl chain (from methyl to butyl), nor the size of the substituent (cf. **8** and **13**), had a significant impact on photophysical properties, except for the fluorescent quantum yield that ranges from 0.80 to 0.95 (Table 3 and Figure 1S in SI). Even the heavy bromine atom in **6** had no influence because of its location far from the BODIPY core. It should be pointed out that for the menthol derivative **8**, with a more constrained structure due to steric hindrance, the fluorescence decay curve is better described as a growing and a decay. Such growing component should be associated with the steric hindrance, which slows down the structural rearrangement upon excitation. Nonetheless slight differences are observed in the fluorescence ability among the aliphatic derivatives. Thus, from methoxy to propoxy the fluorescence quantum yield improves from 0.84 to 0.96 and 0.93 which can be due to the increase of the electron donor character of the alkoxy with the number of methylene units. Accordingly, the merocyanine form is better stabilized and the fluorescence quantum yield is slightly ameliorated. However, a longer aliphatic chain (i.e., butoxy) leads to a more flexible structure, which favors the vibrational decays pathways, as is reflected in the increase in the non-radiative rate constant for compounds **5** (Table 3). Therefore, all these derivatives are characterized by very high fluorescence quantum yields (> 0.80) in all the solvents studied and should be ideal for the vast applications that make use of BODIPYs; i.e., as active media of tunable dye lasers, with the additional advantage of their large Stokes shift ($> 2000\text{ cm}^{-1}$).

Of special interest is the cholesterol derivative **13**. In this case, the BODIPY core was successfully functionalized with a biomolecule, keeping the fluorescence properties of the chromophore unaltered. In brief, a fluorescence marker to monitor biological events has been developed with emission in the blue-green part of the electromagnetic spectrum. This region is not generally used in studies in most of the molecular probes based on BODIPYs (generally from yellow to red).

In addition to alcohols, several phenol derivatives have been prepared. First of all, the phenyl ring did not seem to participate in the delocalized π -system of the indacene core since the spectral band positions were similar to those of the alkoxyBODIPYs (Figure 5); otherwise, a red-shifted emission should have been observed corresponding to an extended delocalization. The optimized geometry revealed that the phenyl ring was twisted with respect to the oxo-BODIPY plane, hampering the electronic coupling (Figure 5). Instead, the lone pair of electrons on oxygen seems to still interact mainly with the BODIPY core, leading to the merocyanine (Figure 4), maintaining the previously discussed blue-shifted spectral bands. However, such hypsochromic shift is slightly lower than the shift in related aliphatic derivatives, as theoretically corroborated by the energy of the frontier orbitals (Figure 2S in SI). This tendency is extrapolated to all phenoxy derivatives, especially those bearing electron withdrawing substituents, like dyes **10** and **11**, which should remove more electronic density from the oxygen (Figure 5). Therefore, the aromatic substituent could slightly remove the electronic density from the oxygen and consequently decrease the extension of the spectral blue-shift.

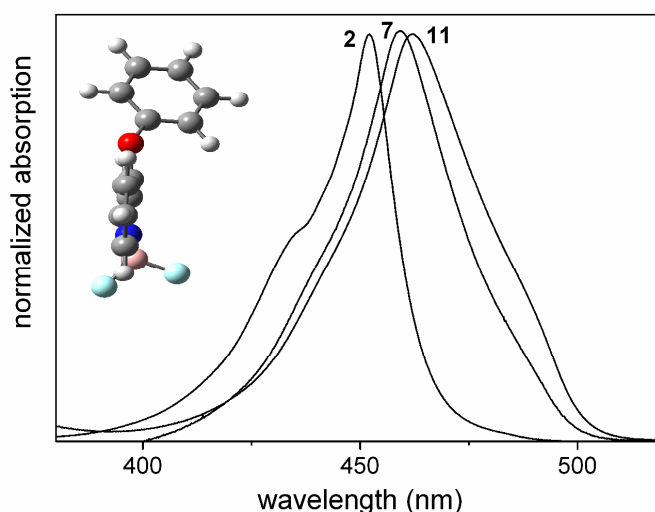


Figure 5. Normalized absorption spectra of BODIPY derivatives bearing methoxy (compound **2**), phenoxy **7**, and *p*-iodophenoxy groups **11** in a common solvent (cyclohexane). The optimized ground state geometry of **7** is also shown.

Table 4 lists the photophysical properties of the aryloxy derivatives of BODIPY. It is worth noticing that derivatives bearing hydroxyl, methoxy or iodine at the phenyl ring were not stable in nucleophilic solvents (such as alcohols or amides). Their photophysical properties change as the solution ages. Probably, this type of solvents act as reactants displacing the initial alkoxy or phenoxy fragments, which may behave as good leaving groups. No effort was made to pursue this observation. For this reason, these solvents were excluded from the photophysical characterization. The phenyl ring in **7** did not affect the fluorescence properties and very high efficiencies were achieved (up to 0.97, Table 4) in all solvents. However, the functionalization of the aryl completely changes the situation. Substitution on the phenyl ring (i.e., **11**, **14**, **9** and **12**), had a drastic effect on the fluorescence properties of the BODIPY, particularly when the substituent was characterized by its electron-releasing ability. Thus, although high fluorescence quantum yields were recorded in apolar media (approaching the unit in most cases), the emission efficiency strongly dropped in polar solvents (Table 4). The exception to this behavior is the formyl substituted derivative **10**, an electron withdrawing group ($\sigma_p = 0.22$) at *para* position of the aryl, where high fluorescence efficiencies are achieved in all considered media, in a similar way to the parent unsubstituted phenyl derivative **7**.

Table 4. Photophysical properties of BODIPYs bearing different aryloxy substituents at the meso position in apolar (cyclohexane) and polar/protic (F3-ethanol) solvents. The complete photophysical data in several solvents are included in Table 2S in SI.

	λ_{ab} (nm)	ϵ_{max} ($10^4 \text{ M}^{-1} \text{ cm}^{-1}$)	λ_{fl} (nm)	ϕ	τ (ns)	k_{fl} (10^8 s^{-1})	k_{nr} (10^8 s^{-1})
<i>c-hexane</i>							
7	459.0	3.5	495.0	0.97	5.78	1.68	0.05
10	466.0	3.8	498.5	0.99	6.03	1.64	0.02

12	458.0	3.4	495.0	0.89	5.84	1.52	0.19
11	462.0	4.7	497.0	0.81	5.66	1.43	0.33
14	458.0	4.2	495.5	0.76	5.25	1.45	0.46
9	457.0	4.9	494.0	0.91	5.60	1.62	0.16
<i>F3-ethanol</i>							
7	449.0	2.9	491.5	0.54	4.71	1.04	1.08
10	456.0	0.7	494.5	0.81	7.68	1.05	0.25
12	448.0	2.9	488.5	0.005	-	-	-
11	452.5	4.0	492.0	0.05	0.33	1.51	28.8
14	448.5	3.6	491.0	0.002	-	-	-
9	448.5	3.8	484.0	0.001	-	-	-

The presence of the electron donor groups methoxy (**9**, $\sigma_p = -0.268$) and hydroxyl (**14**, $\sigma_p = -0.37$) in *ortho* and *para* positions of the phenyl ring, respectively, induced a strong quenching of the fluorescence emission even in low-polarity solvents (e.g., ethyl acetate, Table 2S in SI). This is attributed to the formation of an ICT state that leads to a negligible emission in the polar media (Table 4). Considering the evolution of the fluorescence efficiency with the solvent polarity for compound **11** (bearing a *p*-iodo group) an ICT should also take place in this derivative. The effect of the heavy atom should be very low because of its distant location from the chromophore. However, the iodine behaved like an electron acceptor ($\sigma_p = 0.35$) and the ICT should occur from the BODIPY to the aryl fragment. Furthermore, the quenching effect of the ICT induced by the halogen (compound **11**) is less effective than the above described for compounds **9** and **14**, since higher fluorescence quantum yield are achieved for the former derivative in polar media (Table 4).

Dye **12** is structurally very similar to **13**. Both are functionalized with biomolecules (estrone and cholesterol, respectively), but their photophysical properties are quite different. The presence of cholesterol (cyclohexane attached to oxygen) lead to high fluorescence efficiencies regardless of the media (Table 3); on the other hand, the presence of estrone (phenyl linked to the oxygen) decreases the

1 fluorescence ability of the derivative, especially in polar solvents (Table 4), in concordance with the
2 presence of a quenching ICT state. The phenyl ring can behave as an electron donor or acceptor
3 depending on its substitution pattern, as we have stated before (*i.e.*, donor upon the presence of hydroxyl
4 or acceptor by the attachment of iodine). In **12** the phenyl ring is fused to an aliphatic ring, increasing its
5 electron donor ability, which seems to be high enough as to activate the ICT state.
6
7

8
9 To summarize, BODIPY derivatives bearing aliphatic alkoxy or phenoxy groups are characterized by
10 high fluorescence efficiency in all media. Complementary, the attachment of strong enough electron-
11 donating or withdrawing groups (methoxy, hydroxyl, etc.) at the aryl ring leads to a fluorescence
12 emission sensitive to the environment, making feasible their use as polarity sensors.
13
14

15
16 **X-Ray Structures of 12 and 13.** Cholesterol is a very important organic structure, but previous crystal
17 reports show that it is quite difficult to be solved.¹⁶ Due to this feature, the number of crystal reports is
18 scarce, and in order to modify some properties, functionalization at the OH has been carried out. This
19 modification has an impact in the crystal structure allowing a more efficient packing, therefore
20 upgrading the symmetry from P1 for the non-functionalized cholesterol to P2₁ and even P2₁2₁2₁.¹⁷ For
21 BODIPY **13**, the spatial group is P2₁. Due to the fused polycyclic nature of the cholesterol, no changes in
22 the conformation are observed with the functionalization; however, the alkyl chain attached to it has
23 more freedom which allows it to acquire the better orientation to maximize the packing.
24
25

26
27 As observed in other BODIPY systems,⁷ the O-C_{BODIPY} distance is shorter than the O-C_{chol} distance due
28 to the merocyanine character of this oxygen (Figure 4). The distances on the BODIPY moiety are not
29 statistically differentiable due to the equivalent resonance structures in the conjugate system. There is a
30 small dihedral angle of 5.7° between the pyrrole rings, but the BODIPY moiety could be considered as
31 planar. Cholesterol is tilted from this plane about 39° (Figure 6).
32
33
34
35
36
37
38
39
40
41
42
43
44
45
46
47
48
49
50
51
52
53
54
55
56
57
58
59
60

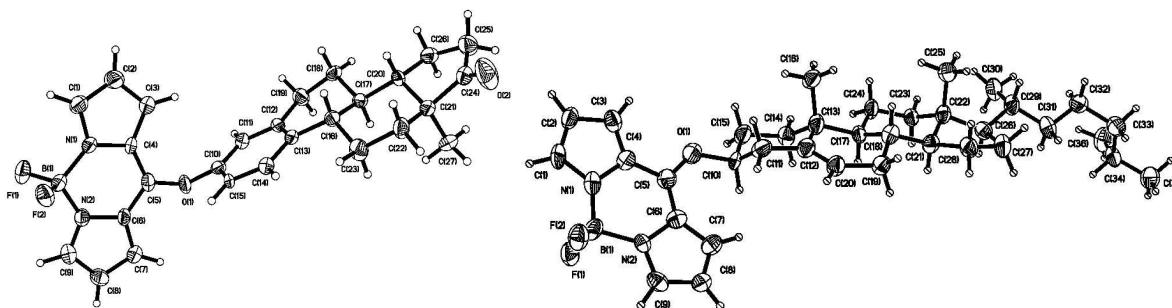


Figure 6. Conformations adopted in the crystal for compounds **12** (left) and **13** (right). The ellipsoids were drawn at 50% of probability level.

The crystal packing is bilayer type, expected because of the amphiphilic character of this derivative (Figure 7). The short contact distances $H\cdots H$ in the cholesterol moiety range from 2.16 to 2.37 Å, showing that these contacts albeit being unfavorable (considering the London forces) are present due to the stabilization energy introduced by the BODIPY fragment. The BODIPY moieties are arranged in a parallel fashion (Figure 7), although it will not be a π - π interaction because the interplanar distance is 3.34 Å, but the offset is ~ 3.0 Å. The most important interactions are the ones formed by one of the fluorine atoms which behaves as a bidentate HB acceptor ($C3-H3\cdots F1 = 2.53$ Å and $C11-H11B\cdots F1 = 2.65$ Å)¹⁸ generating a 2-D layer (the BODIPY layer or polar domain).

The conformation of the estrone moiety remains unchanged in BODIPY **12** (Figure 6). It can be compared to the reported structure of the unfunctionalized estrone by Busetta *et al.*¹⁹ however, the functionalization in this case, in contrast to that of cholesterol, reduces the symmetry of the crystal bringing it from $P2_12_12_1$ to $P2_1$, because of the elimination of the hydroxyl group and further removal of the intramolecular HB between it and the carbonyl group.

The other difference with respect to derivative **13** is the size, estrone is smaller, then the hydrophobic character is not as strong as in **13**, therefore the packing is different. On this derivative the bilayer arrangement is not the favored one, but a zig-zag chain arrangement (Figure 7). But as in **13**, the strongest interactions are formed by the F atoms, in this case both F atoms participate in the HB

generating the 3-D structure [$C7-H7 \cdots F1 = 2.36 \text{ \AA}$, $C22-H22 \cdots F2 = 2.52 \text{ \AA}$ and $C2-H2 \cdots F2 = 2.60 \text{ \AA}$].²⁰ In addition, the tilt of the BODIPY moiety against the estrone mean plane is 79.6° .

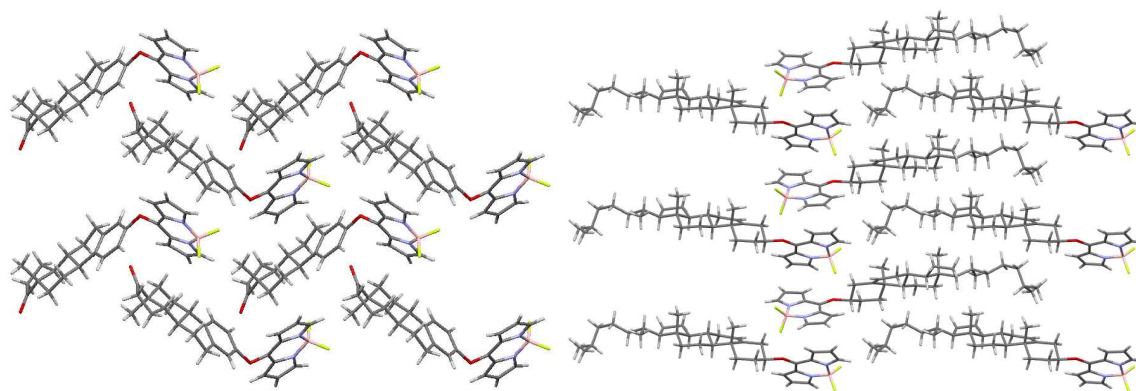


Figure 7. Crystal packing of **12** (left) and **13** (right) showing the difference between them due to size of cholesterol in comparison to estrone

Conclusions

We have successfully prepared a family of 8-alkoxy- and 8-aryloxyBODIPY dyes in a straightforward manner in moderate to good yields. The substituents at the meso position carry functional groups that will allow further elaboration for specific applications. Four biomolecules (eugenol, menthol, cholesterol and estrone) were easily attached to the BODIPY core, which demonstrates the usefulness of this method to label biologically relevant molecules.

The inclusion of heteroatoms at the central position of the BODIPY is an adequate strategy to achieve BODIPY-based blue-green emitting fluorophores. Furthermore, the proper election of the heteroatom, in terms of its electronegativity, allows the modulation of the extension of the blue-shift. Accordingly, the amino group induces a more pronounced spectral shift to higher energies than the alkoxy group. However, the fluorescence performance of the mono and disubstituted 8-aminoBODIPYs were limited in polar media. Herein, we show that 8-alkoxyBODIPYs overcome such problem and display high fluorescence efficiencies irrespective of the media. The lower electron donor character of the alkoxy,

with regard to the amino group, prevents the formation of quenching intramolecular charge transfer states, which limits the fluorescence performance of the latter dyes in polar media. Of course, the inclusion of electron donor or acceptor substituents at the oxygen fragment can also lead to the formation of the ICT state, with the consequent reduction in the fluorescence efficiency.

Summing up, BODIPY dyes bearing heteroatoms (N and O) allow for a wide coverage of the visible electromagnetic region (from yellow to blue). Taking into account the reported BODIPYs with red-shifted emission, it is in fact possible to span the whole visible spectrum, by just choosing the adequate modification of the chromophoric core.

Experimental.

Photophysical properties. The photophysical properties were registered in diluted solutions (around 2×10^{-6} M), prepared by adding the corresponding solvent to the residue from the adequate amount of a concentrated stock solution in acetone, after vacuum evaporation of this solvent. The fluorescence spectra were corrected from the wavelength dependence of the detector sensibility. Fluorescence quantum yield (ϕ) was obtained using a 0.1 M NaOH aqueous solution of fluorescein ($\phi^r = 0.79$) as reference and corrected by the different refractive index of the solvent used for the sample and the reference. Radiative decay curves were registered with the time correlated single-photon counting technique using a microchannel plate detector, with picosecond time resolution (~ 20 ps). Fluorescence emission was monitored at the maximum emission wavelength after excitation at 440 nm by means of a diode laser with 150 ps FWHM pulses. The fluorescence lifetime (τ) was obtained from the slope after the deconvolution of the instrumental response signal from the recorded decay curves by means of an iterative method. The goodness of the exponential fit was controlled by statistical parameters (chi-square, Durbin-Watson and the analysis of the residuals). The radiative (k_f) and non-radiative deactivation (k_{nr}) rate constants were calculated by means of: $k_f = \phi/\tau$ and $k_{nr} = (1-\phi)/\tau$, respectively.

Theoretical calculations. Ground state geometry was optimized by the hybrid DFT method B3LYP, using the double-valence basis set (6-31G), as implemented in Gaussian 09. The geometry was considered as a minimum of energy after the analysis of the frequencies did not yield any negative value.

X-ray diffraction measurements. Each crystal was mounted on a glass fiber using paratone, and its crystal data was acquired at room temperature and it was with the suite APEX 2.²¹ The solution was obtained through direct methods. Absorption corrections were applied. The Hydrogens were placed by geometry and they were restrained to ride on the heavy atoms.

Synthesis and characterization: ¹H and ¹³C NMR spectra were recorded on a 200 MHz spectrometer in deuteriochloroform (CDCl₃), with either tetramethylsilane (TMS) (0.00 ppm ¹H, 0.00 ppm ¹³C), chloroform (7.26 ppm ¹H, 77.00 ppm ¹³C), acetonitrile-*d*₃ (1.94 ppm ¹H, 118.3, 1.3 ppm ¹³C), or acetone-*d*₆ (2.05 ppm ¹H, 206.0, 29.8 ppm ¹³C) as internal reference. Data are reported in the following order: chemical shift in ppm, multiplicities (br (broadened), s (singlet), d (doublet), t (triplet), q (quartet), sex (sextet), hep (heptet), m (multiplet), exch (exchangeable), app (apparent)), coupling constants, J (Hz), and integration. Infrared spectra were recorded on a FTIR spectrophotometer. Mass spectrometry data were collected on TOF analyzer. Peaks are reported (cm⁻¹) with the following relative intensities: s (strong, 67–100 %), m (medium, 40–67%), and w (weak, 20–40%). Melting points are not corrected.

Typical method 1 (TM1). A Schlenk tube equipped with a stir bar under N₂ was charged with BODIPY **1** (0.10 g, 0.42 mmol, 1 equiv.). The corresponding alcohol (5 mL) was added and the mixture was stirred until the solids dissolved. The mixture was purged with N₂ for 5 min whereupon CuTC (0.119 g, 0.63 mmol, 1.5 equiv.) and Na₂CO₃ (0.07 g, 0.63 mmol, 1.5 equiv.) were added. The Schlenk tube was immersed in a pre-heated oil-bath at 55 °C and the stirring continued until the consumption of the starting material. The solvent was removed *in vacuo* and the crude material was adsorbed in SiO₂ gel. The product was purified by column chromatography using a hexane/EtOAc gradient. For purposes of characterization, the products were crystallized from CH₂Cl₂/hexanes.

Typical method 2 (TM2). A Schlenk tube equipped with a stir bar under N₂ was charged with BODIPY **1** (0.10 g, 0.42 mmol, 1 equiv) and CH₃CN (6 mL). The mixture was purged with N₂ for 5 min whereupon CuTC (0.119 g, 0.63 mmol, 1.5 equiv.) and the corresponding alcohol or phenol was added

(0.63 mmol, 1.5 eq.). The reaction mixture was stirred for 5 min. upon which Na₂CO₃ (0.07 g, 0.63 mmol, 1.5 equiv.) was added. The Schlenk tube was immersed in a pre-heated oil-bath at 55 °C and the stirring continued until the consumption of the starting material. The solvent was removed *in vacuo* and the crude material was adsorbed in SiO₂ gel. The product was purified by column chromatography using a hexane/EtOAc gradient. For purposes of characterization, the products were crystallized from CH₂Cl₂/hexanes.

BODIPY 2. Following TM1. The product (68.5 mg, 73%) was obtained as a yellow solid. R_f = 0.3 (30% EtOAc/Hexanes). Mp 137-139 °C. IR KBr (cm⁻¹) 3127 (w), 3116 (w), 2925 (w), 1739 (w), 1559 (s), 1533 (s), 1465 (s), 1395 (s), 1366 (s), 1335 (m), 1291 (s), 1263 (s), 1231 (s), 1186 (m), 1131 (s), 1085 (s), 1002 (m), 971 (s), 938 (m), 866 (w), 779 (m), 730 (m), 647 (m), 551 (w), 443 (w). ¹H CDCl₃ (300 MHz) δ 7.74 (s, 2H), 7.37 (d, J = 6.0 Hz, 2H), 6.54 (s, 2H), 4.49 (s, 3H); ¹³C CDCl₃(75 MHz) δ 162.00, 139.58, 126.22, 125.52, 116.69, 62.15.^{13a}

BODIPY 3. Following TM1. The product (62.0 mg, 62%) was obtained as a yellow solid. R_f = 0.5 (30% EtOAc/hexanes). Mp 118-119 °C. IR KBr (cm⁻¹) 2925 (w), 1736, (w), 1558 (s), 1529 (m), 1474 (w), 1445 (s), 1402 (s), 1351 (m), 1331 (m), 1292 (s), 1262 (s), 1232 (m), 1151 (m), 1132 (s), 1100 (s), 1073 (s), 1008 (m), 960 (s), 787 (w), 861 (w), 763 (m), 728 (m), 643 (w), 582 (w), 435 (w). ¹H CDCl₃ (300 MHz) δ 7.66 (s, 2H), 7.27 (d, J = 3.6 Hz, 2H), 6.45 (d, J = 1.8 Hz, 2H), 4.68 (q, J = 7.2 Hz, 2H), 1.54 (t, J = 6.9 Hz, 3H); ¹³C CDCl₃(75 MHz) δ 161.62, 139.371, 126.54, 125.54, 116.54, 71.51, 15.51. HRMS FABS (M+H⁺) Calcd for C₁₁H₁₂BF₂N₂O: 237.1011. Found: 237.1015.

BODIPY 4. Following TM1. The product (73.5 mg, 70%) was obtained as a yellow solid. R_f = 0.4 (30% EtOAc/hexanes). Mp 99-100 °C. IR KBr (cm⁻¹) 3123 (w), 2972 (w), 2885 (w), 1730 (w), 1554 (s), 1471 (m), 1441 (s), 1399 (s), 1365 (m), 1333 (w), 1290 (m), 1264 (s), 1225 (s), 1151 (m), 1130 (s), 1096 (s), 1079 (s), 1040 (m), 995 (w), 970 (s), 862 (w), 769 (s), 728 (s), 644 (m), 583 (w), 453 (w). ¹H CDCl₃ (300 MHz) δ 7.73 (s, 2H), 7.34 (d, J = 3.6 Hz, 2H), 6.51 (d, J = 3.6 Hz, 2H), 4.66 (t, J = 6.0 Hz,

2H), 1.98 (m, 2H), 1.13 (t, $J = 7.2$ Hz, 2H); ^{13}C CDCl_3 (75 MHz) δ 161.893, 139.45, 125.47, 116.53, 77.78, 23.395, 10.662. HRMS FABS ($\text{M}+\text{H}^+$) Calcd for $\text{C}_{12}\text{H}_{14}\text{BF}_2\text{N}_2\text{O}$: 251.1167. Found: 251.1171.

BODIPY 5. Following TM2. The product (74.3 mg, 67%) was obtained as yellow crystals. $R_f = 0.6$ (30% EtOAc/hexanes). Mp 79–80 °C. IR (KBr, cm^{-1}) 3125 (w), 2963 (w), 1565 (s), 1474 (w), 1438 (m), 1405 (s), 1368 (w), 1350 (w), 1262 (s), 1226 (m), 1127 (m), 1094 (s), 1076 (m), 1043 (m), 992 (w), 968 (m), 768 (m), 730 (m). ^1H NMR (300 MHz, CDCl_3) δ 7.71 (s, 2H), 7.32 (s, 2H), 6.50 (s, 2H), 4.68 (m, $J = 5.7$ Hz, 2H), 1.93 (m, $J = 6.6$ Hz, 2H), 1.56 (m, $J = 7.2$ Hz, 2H), 1.03 (m, $J = 6.6$ Hz, 2H); ^{13}C NMR (75 MHz, CDCl_3) δ 161.8, 139.3, 126.5, 125.5, 116.5, 75.4, 31.8, 19.3, 13.9. HRMS FABS ($\text{M}+\text{H}^+$) Calcd for $\text{C}_{13}\text{H}_{16}\text{BF}_2\text{N}_2\text{O}$: 265.1324. Found: 265.1320.

BODIPY 6. Following TM2. The product (87.5 mg, 66%) was obtained as a bright yellow solid. $R_f = 0.4$ (30% EtOAc/hexanes). Mp 120.5–122.0 °C. IR KBr (cm^{-1}) 2975 (w), 2940, (w), 2634 (w) 1709 (s), 1649 (s), 1545 (s), 1460 (m), 1422 (s), 1402 (m), 1365 (m), 1311 (w), 1276 (m), 1090 (s), 1012 (m), 982 (m), 967 (w), 946 (m), 778 (m), 759 (m), 646 (w), 660 (m), 586 (w). ^1H CDCl_3 (200 MHz) δ 7.77 (s, 1H), 7.35 (d, $J = 4.0$ Hz, 2H), 6.55 (s, 2H), 4.99 (t, $J = 6$ Hz, 2H), 3.77 (t, $J = 6$ Hz, 2H); ^{13}C CDCl_3 (75 MHz) δ 160.30, 140.23, 126.38, 125.88, 74.01, 2810. HRMS FABS ($\text{M}+\text{H}^+$) Calcd for $\text{C}_{11}\text{H}_{11}\text{BBBrF}_2\text{N}_2\text{O}$: 315.0116. Found: 315.0119.

BODIPY 7. Following TM2. The product (107.5 mg, 90%) was obtained as a bright yellow solid. $R_f = 0.67$ (30% EtOAc/hexanes). Mp 129.8–131.4 °C. IR KBr (cm^{-1}) 3122 (w), 1740 (w), 1573 (s), 1526 (m), 1486 (m), 1398 (s), 1364 (s), 1332 (w), 1283 (s), 1251 (s), 1225 (s), 1187 (w), 1118 (s), 1073 (s), 1040 (s), 960 (s), 868 (w), 786 (m), 768 (s), 721 (m), 694 (m), 638 (m), 568 (w), 478 (w). ^1H CDCl_3 (300 MHz) δ 7.74, (s, 2H); 7.52–7.47 (t, 2H, $J = 7.32$ Hz); 7.41–7.36 (t, 1H, $J = 7.32$ Hz); 7.24 (s, 2H); 6.67 (s, 2H); 6.39 (s, 2H); ^{13}C CDCl_3 (75 MHz) δ 156.04, 141.08, 130.85, 130.85, 127.33, 126.457, 120.44, 117.08.^{13a}

BODIPY 8. Following TM2. The product (76.7 mg, 53%) was obtained as a light olive green solid. $R_f = 0.4$ (30% EtOAc/hexanes). Mp 149.4–250.4 °C. IR KBr (cm^{-1}) 2944 (m), 2871 (m), 1550 (s), 1469 (m), 1428 (s), 1407 (s), 1322 (m), 1290 (m), 1256 (s), 1223 (s), 1186 (w), 1147 (w), 1126 (s),

1094 (s), 1076 (s), 1052 (m), 963 (s), 847 (w), 781 (m), 766 (m), 734 (m), 676 (w), 64 (m), 585 (w), 525 (w). ^1H CDCl_3 (300 MHz) δ 7.71 (s, 2H), 7.28 (s, 2H), 6.52 (s, 2H), 4.97 (m, 1H), 2.37 (d, J = 12.3 Hz, 1H), 2.09-0.745 (m, 17H); ^{13}C CDCl_3 (75 MHz) δ 161.42, 139.03, 126.61, 124.88, 116.528, 85.56, 48.86, 40.01, 34.27, 31.77, 27.01, 24.08, 22.22, 20.78, 17.01. HRMS FABS ($\text{M}+\text{H}^+$) Calcd for $\text{C}_{19}\text{H}_{26}\text{BF}_2\text{N}_2\text{O}$: 347.2106. Found: 347.2104.

BODIPY 9. Following TM2. The product (77.3 mg, 52%) was obtained as a yellow solid. R_f = 0.7 (30% EtOAc/hexanes). Mp 273-274 °C. IR (KBr, cm^{-1}) 3130 (w), 1637 (s), 1612 (m), 1569 (s), 1540 (s), 1513 (m), 1461 (m), 1413 (s), 1395 (s), 1380 (s), 1267 (m), 1235 (w), 1117 (m), 1032 (m), 944 (w), 792 (m). ^1H NMR (300 MHz, CDCl_3) δ 7.71 (s, 2H), 7.15 (d, J = 9 Hz, 1H), 6.88 (d, J = 3 Hz, 2H), 6.70 (d, J = 3 Hz, 2H), 6.37 (d, J = 3 Hz, 2H), 6.05-5.96 (m, 1H), 5.17-5.11 (m, J = 9 Hz, 2H), 3.72 (s, 3H), 3.46 (d, J = 6 Hz, 2H); ^{13}C NMR (75 MHz, CDCl_3) δ 160.8, 150.6, 142.6, 141.0, 140.3, 136.8, 126.7, 125.5, 121.7, 121.5, 116.9, 116.7, 114.1, 56.3, 40.3. HRMS FABS ($\text{M}+\text{H}^+$) Calcd for $\text{C}_{19}\text{H}_{18}\text{BF}_2\text{N}_2\text{O}_2$: 355.1429. Found: 355.1423.

BODIPY 10. Following TM2. The product (53.6 mg, 41%) was obtained as a bright yellow solid. R_f = 0.4 (30% EtOAc/hexanes). Mp 195 °C (dec). IR KBr (cm^{-1}) 3114 (w), 2857 (w), 1695 (m), 1597 (m), 1565 (s), 1495 (m), 1473 (m), 1407 (s), 1395 (s), 1365 (m), 1332 (w), 1287 (m), 1255 (s), 1226 (s), 1202 (m), 1158 (w), 1124 (s), 1088 (s), 1065 (s), 1044 (m), 954 (s), 874 (w), 849 (w), 775 (m), 766 (m), 724 (w), 638 (w), 607 (w), 577 (w), 504 (w). ^1H CDCl_3 (300 MHz) δ 10.04 (s, 1H), 8.01 (d, J = 8.4 Hz), 7.80 (s, 2H), 7.41 (d, J = 8.7 Hz), 6.82 (s, 2H), 6.46 (s, 2H); ^{13}C CDCl_3 (75 MHz) δ 189.16, 159.96, 141.35, 133.22, 131.06, 126.46, 125.45, 118.99, 116.57. HRMS FABS ($\text{M}+\text{H}^+$) Calcd for $\text{C}_{16}\text{H}_{12}\text{BF}_2\text{N}_2\text{O}_2$: 313.0960. Found: 313.0963.

BODIPY 11. Following TM2. The product (98.1 mg, 57%) was obtained as yellow crystals. R_f = 0.6 (30% EtOAc/hexanes.). Mp 122-124 °C. IR (KBr, cm^{-1}) 3130 (w), 3109 (w), 2865 (w), 2353 (m), 2342 (m), 1569 (s), 1541 (s), 1414 (s), 1400 (s), 1263 (s), 1155 (m), 1120 (s), 1082 (s), 1053 (m), 1000 (w), 977 (m). ^1H NMR (200 MHz, CDCl_3) δ 7.79 (d, J = 9 Hz, 2H), 7.02 (d, J = 9 Hz, 2H), 6.75 (d, J =

3.6 Hz, 2H), 6.43 (s, 2H); ^{13}C NMR (75 MHz, CDCl_3) δ 156.2, 141.7, 138.8, 128.1, 126.6, 122.3, 117.5, 114.3, 90.8. HRMS FABS ($\text{M}+\text{H}^+$) Calcd for $\text{C}_{15}\text{H}_{11}\text{BF}_2\text{IN}_2\text{O}$: 410.9977. Found: 410.9975.

BODIPY 12. Following TM2. The product (147.0 mg, 76%) was obtained as yellow crystals. R_f = 0.36 (30% EtOAc/hexanes). Mp 202-204 °C. IR (KBr, cm^{-1}) 3120 (w), 3066 (w), 2943 (m), 2865 (w), 1718 (s), 1619 (w), 1582 (w), 1567 (s), 1538 (s), 1462 (m), 1409 (s), 1400 (s), 1380 (m), 1356 (w), 1287 (m), 1259 (s), 1165 (s), 1157 (w), 1115 (s), 970 (m). ^1H NMR (300 MHz, CDCl_3) δ 7.72 (s, 2H), 7.37 (d, J = 7.8 Hz, 1H), 7.00 (m, J = 7.8 Hz, 1H), 6.97 (s, 1H), 6.72 (s, 2H), 6.39 (s, 2H), 2.91 (s, 3H), 2.58 - 2.35 (m, 4H), 2.20 - 2.02 (m, 6H), 1.98 - 1.463 (m, 9H), 0.90 (s, 3H); ^{13}C NMR (75 MHz, CDCl_3) δ 207.5, 159.9, 153.9, 140.8, 139.7, 139.0, 132.0, 127.6, 126.3, 120.0, 116.9, 115.6, 113.2, 50.8, 48.3, 44.4, 38.2, 36.2, 36.1, 31.8, 29.7, 26.5, 21.9, 14.2. HRMS FABS ($\text{M}+\text{H}^+$) Calcd for $\text{C}_{27}\text{H}_{28}\text{BF}_2\text{N}_2\text{O}_2$: 461.2212. Found: 461.2215.

BODIPY 13. Following TM2. The product (145.2 mg, 60%) was obtained as yellow crystals. R_f = 0.7 (30% EtOAc/hexanes,). Mp 171–173 °C. IR (KBr, cm^{-1}) 2938 (w), 2893 (w), 2865 (w), 1738 (w), 1668 (w), 1565 (s), 1471 (w), 1431 (s), 1400 (s), 1371 (w), 1341 (w), 1290 (m), 1263 (s), 1225 (m), 1151 (w), 1126 (m), 1095 (s), 1075 (s), 1053 (w), 1000 (w), 972 (m), 766 (m), 728 (m). ^1H NMR (300 MHz, CDCl_3) δ 7.62 (s, 2H), 7.19 (s, 2H), 6.42 (s, 2H), 5.4 (s, 1H), 2.57 (d, J = 6 Hz, 2H), 2.134 - 0.765 (m), 0.62 (s, 3H); ^{13}C NMR (75 MHz, CDCl_3) δ 160.9, 139.3, 138.8, 133.4, 132.3, 127.9, 126.9, 125.2, 124.4, 123.1, 116.6, 85.0, 75.3, 57.0, 56.5, 50.4, 42.6, 39.9, 38.9, 37.2, 36.5, 36.1, 32.2, 30.0, 28.2, 24.6, 24.2, 23.1, 21.4, 19.7, 19.0, 12.2. HRMS FABS ($\text{M}+\text{H}^+$) Calcd for $\text{C}_{36}\text{H}_{52}\text{BF}_2\text{N}_2\text{O}$: 577.4141. Found: 577.4139.

BODIPY 14. Following TM2. The product (70.5 mg, 56%) was obtained as yellow crystals. R_f = 0.4 (30% EtOAc/hexanes,). Mp 198-200 °C. IR (KBr, cm^{-1}) 3506 (w), 3129 (w), 1601 (w), 1568 (s), 1503 (s), 1399 (s), 1366 (m), 1289 (m), 1256 (s), 1230 (s), 1216 (w), 1188 (m), 1113 (s), 1088 (s), 1013 (m), 946 (w), 930 (m), 842 (w), 762 (s). ^1H NMR (200 MHz, CDCl_3) δ 7.7 (s, 2H), 7.12 (d, J = 9 Hz, 2H), 6.92 (d, J = 9 Hz, 2H), 6.70 (m, J = 4 Hz, 2H), 6.40 (d, J = 4 Hz, 2H); ^{13}C NMR (75 MHz, CDCl_3) δ

154.9, 149.2, 140.7, 128.1, 126.4, 121.6, 117.2, 117.01, 116.5. HRMS FABS (M+H⁺) Calcd for C₁₅H₁₂BF₂N₂O₂: 301.0960. Found: 301.0964.

Acknowledgements

We thank CONACyT (Grant 129572) for financial support. J. O. F.-R., C. A. O.-M., and C. F. A. G.-D. thank CONACyT for graduate scholarships. The Gobierno Vasco is thanked for a PhD contract (Ixone Esnal, IT339-10) and by financial support (SPE11UN064 and SPE12UN140). Welch Foundation Houston, Texas (Grant # 0546) is also acknowledged. We also thank Cuantico de Mexico for donation of **1**.

Supporting Information Available: Copies of the ¹H and ¹³C NMR spectra of all the compounds described, full photophysical data in several solvents, calculated energies of the frontier orbitals, tables of atom coordinates and absolute energies. This material is available free of charge via the Internet at <http://pubs.acs.org>.

References

- (1) (a) Sharma, A.; Neibert, K.; Sharma, R.; Hourani, R.; Maysinger, D.; Kakkar, A. *Macromolecules* **2011**, *44*, 521. (b) Caldorera-Moore, M. E.; Liechty, W. B.; Peppas, N. A. *Acc. Chem. Res.* **2011**, *44*, 1061.
- (2) Bura, T.; Leclerc, N.; Fall, S.; Lévesque, P.; Heiser, T.; Retailleau, P.; Rihn, S.; Mirloup, A.; Ziessel, R. *J. Am. Chem. Soc.* **2012**, *134*, 17404.
- (3) Haugland, R. P. *The Handbook. A Guide to Fluorescent Probes and Labeling Technology*, 10th Edn, Molecular Probes Inc., Eugene, Oregon, 2005 USA.
- (4) (a) Ziessel, R.; Ulrich, G.; Harriman, A. *New J. Chem.* **2007**, *31*, 496. (b) Ulrich, G.; Ziessel, R.; Harriman, A. *Angew. Chem, Int. Ed.* **2008**, *47*, 1184. (c) Benniston, A. C.; Copley, G. *Phys. Chem. Chem. Phys.* **2009**, *11*, 4124. (d) Loudet, A.; Burgess, K. *Chem. Rev.* **2007**, *107*, 4891. (e) Wood, T. E.; Thompson, A. *Chem Rev.* **2007**, *107*, 1831.
- (5) (a) Han, J.; Loudet, A.; Barhoumi, B.; Burghardt, R. C.; Burgess, K. *J. Am. Chem. Soc.* **2009**, *131*, 1642. (b) Kamiya, M.; Johnsson, K. *Anal. Chem.* **2010**, *82*, 6472. (c) Li, Z.; Mintzer, E.; Bittman, R. *J. Org. Chem.* **2006**, *71*, 1718. (d) Ariola, F. S.; Li, Z.; Cornejo, C.; Bittman, R.; Heikal, A. A. *Biophys. J.* **2009**, *96*, 2696. (e) Li, Z.; Bittman, R. *J. Org. Chem.* **2007**, *72*, 8376. (f) Ehenschwender, T.; Wagenknecht, H.-A. *J. Org. Chem.* **2011**, *76*, 2301. (g) Kim, D.-R.; Ahn, H.-C.; Leec, W.-J.; Ahn, D.-R. *Chem. Commun.* **2011**, *47*, 791. (h) Hornillos, V.; Carrillo, E.; Rivas, L.; Amat-Guerri, F.; Acuña, A.

U. *Bioorg. Med. Chem. Lett.* **2008**, *18*, 6336. (i) Ojida, A.; Sakamoto, T.; Inoue, M.-a.; Fujishima, S.-h.; Lippens, G.; Hamachi, I. *J. Am. Chem. Soc.* **2009**, *131*, 6543. (j) Krumova, K.; Oleynik, P.; Karam, P.; Cosa, G. *J. Org. Chem.* **2009**, *74*, 3641. (k) Kowada, T.; Kikuta, J.; Kubo, A.; Ishii, M.; Maeda, H.; Mizukami, S.; Kikuchi, K. *J. Am. Chem. Soc.* **2011**, *133*, 17772. (l) Gonçalves, M. S. T. *Chem. Rev.* **2009**, *109*, 190.

(6) (a) Camerel, F.; Ulrich, G.; Barberá, J.; Ziesse, R. *Chem. Eur. J.* **2007**, *13*, 2189. (b) Warnan, J.; Buchet, F.; Pellegrin, Y.; Blart, E.; Odobel, F. *Org. Lett.* **2011**, *13*, 3944. (c) Ziesse, R.; Harriman, A. *Chem. Commun.* **2011**, *47*, 611. (d) Gust, D.; Moore, T. A.; Moore, A. L. *Acc. Chem. Res.* **2009**, *42*, 1890. (e) Rousseau, T.; Cravino, A.; Bura, T.; Ulrich, G.; Ziesse, R.; Roncali, J. *Chem. Commun.* **2009**, 1673. (f) Zrig, S.; Rémy, P.; Andrioletti, B.; Rose, E.; Asselberghs, I.; Clays, K. *J. Org. Chem.* **2008**, *73*, 1563. (g) Alamiry, M. A. H.; Benniston, A. C.; Copley, G.; Elliott, K. H.; Harriman, A.; Stewart, B.; Zhi, Y.-G. *Chem. Mater.* **2008**, *20*, 4024. (h) Bozdemir, A.; Büyükcakir, O.; Akkaya, E. U. *Chem. Eur. J.* **2009**, *15*, 3843. (i) Warnan, J.; Pellegrin, Y.; Blart, E.; Odobel, F. *Chem. Commun.* **2012**, *48*, 675. (j) Xiao, Y.; Zhang, D.; Qian, X.; Costela, A.; Garcia-Moreno, I.; Martin, V.; Perez-Ojeda, M. E.; Bañuelos, J.; Gartzia, L.; López Arbeloa, I. *Chem. Commun.* **2011**, *47*, 11513.

(7) Goud, T. V.; Tutar, A.; Biellmann, J.-F. *Tetrahedron* **2006**, *62*, 5084.

(8) (a) Prokopcová, H.; Kappe, C. O. *Angew. Chem. Int. Ed.* **2008**, *47*, 3674. (b) Prokopcová, H.; Kappe, C. O. *Angew. Chem. Int. Ed.* **2009**, *48*, 2276.

(9) (a) Peña-Cabrera, E.; Aguilar-Aguilar, A.; Gonzalez-Dominguez, M.; Lager, E.; Zamudio-Vazquez, R.; Godoy-Vargas, J.; Villanueva-García, F. *Org. Lett.* **2007**, *9*, 3985. (b) Arroyo, I. J.; Hu, R.; Tang, B. Z.; López, F. I.; Peña-Cabrera, E. *Tetrahedron* **2011**, *67*, 7244.

(10) Arroyo, I. J.; Hu, R.; Merino, G.; Tang, B. Z.; Peña-Cabrera, E. *J. Org. Chem.* **2009**, *74*, 5719.

(11) (a) Gómez-Durán, C. F. A.; García-Moreno, I.; Costela, A.; Martin, V.; Sastre, R.; Bañuelos, J.; López Arbeloa, F.; López Arbeloa, I.; Peña-Cabrera E. *Chem. Comm.* **2010**, *46*, 5103. (b) Bañuelos, J.; V. Martín, V.; Gómez-Durán, C. F. A.; Arroyo-Cordoba, I. J.; Peña-Cabrera, E.; García-Moreno, I.; Costela, A.; Pérez-Ojeda, M. A.; Arbeloa, T.; López Arbeloa, I. *Chem. Eur. J.* **2011**, *17*, 7261. (c) Osorio-Martínez, C. A.; Urías-Benavides, A.; Gómez-Durán, C. F. A.; Bañuelos, J.; Esnal, I.; López Arbeloa, I.; Peña-Cabrera, E. *J. Org. Chem.* **2012**, *77*, 5434.

(12) (a) Kasurinen, J. *Biochem. Biophys. Res. Commun.* **1992**, *187*, 1594. (b) Ellena, J. F.; Le, M.; Cafiso, D. S.; Solis, R. M.; Langston, M.; Sankaram, M. B. *Drug Delivery* **1999**, *6*, 9. (c) Hendrickson, H. S.; Hendrickson, E. K.; Johnson, I. D.; Farber, S. A. *Anal. Biochem.* **1999**, *276*, 27. (d) Dahim, M.;

- Mizuno, N. K.; Li, X.-M.; Momsen, W. E.; Momsen, M. M.; Brockman, H. L. *Biophys. J.* **2002**, *83*, 1511. (e) Kaiser, R. D.; London, E. *Biochim. Biophys. Acta* **1998**, *1375*, 13.
- (13) (a) Leen, V.; Yuan, P.; Wang, L.; Boens, N.; Dehaen, W. *Org Lett.* **2012**, *14*, 6150. (b) Wang, L.; Zhang, Y.; Xiao, Y. *RSC Adv.* **2013**, *3*, 2203.
- (14) (a) Masamune, S.; Hayase, Y.; Schilling, W.; Chan, W.-K.; Bates, G. S. *J. Am Chem. Soc.* **1977**, *99*, 6756. (b) Masamune, S.; Kamata, S.; Schilling, W. *J. Am. Chem. Soc.* **1975**, *97*, 3515.
- (15) Musaev, D. G.; Liebeskind, L. S. *Organometallics* **2009**, *28*, 4639.
- (16) (a) Shieh, H.-S.; Hoard, L.G.; Nordman, C. E. *Acta Crystallogr.* **1981**, *37B*, 1538. (b) Hsu, L.-Y.; Kampf, J. W.; Nordman, C. E. *Acta Crystallogr B*, **2002**, *58*, 260.
- (17) In the following references the CCDC code is given first followed by the spatial group in square brackets and then the corresponding reference. [SEGPID, P1] Polishchuk, A. P.; Yu, M.; Antipin, T. V.; Timofeeva, O. D.; Lavrentovich, A. S.; Kotel'chuk, L.A.; Taraborkin, L. A.; Struchkov, T. *Kristallografiya (Russ.) (Crystallogr. Rep.)* **1988**, *33*, 1134. [VAVBUR, P1] Ikonen, S.; Jurcek, O.; Wimmer, Z.; Drasar, P.; Kolehmainen, E. *J. Mol. Struct.* **2012**, *1011*, 25. [DECHUO, P2₁] Polishchuk, A. P.; Antipin, M.; Timofeeva, T. V.; Yu, T.; Struchkov, V.; Kulishov, I. *Khim. Fiz. (Russ.) (Sov. J. Chem. Phys.)* **1985**, *4*, 329. [FELBII, P2₁] Powell, D. A.; Maki, T.; Fu, G. C. *J. Am. Chem. Soc.* **2005**, *127*, 510. [JABZER, P2₁] Suh, I.-H.; Ko, T.-S.; Park, Y. J.; Yoon, Y. K.; Saenger, W. *Acta Crystallogr.* **1988**, *C44*, 2163. [KOGPUR, P2₁] Polishchuk, A. P.; Timofeeva, T. V.; Yu. M.; Antipin; Gerr, R. G.; Kulishov, V. I.; Struchkov, T.; Payusova, I. K.; Tolmachev, A. V. *Zh. Strukt. Khim. (Russ.) (J. Struct. Chem.)* **1990**, *31*, 67-5. [SEGPOJ, P2₁] Polishchuk, A. P.; Yu, M.; Timofeeva, T. V.; Lavrentovich, O. D.; Kotel'chuk, A. S.; Taraborkin, L. A.; Struchkov, Y. T. *Kristallografiya (Russ.) (Crystallogr. Rep.)* **1988**, *33*, 1134. [SUBHOM, P2₁2₁2₁] Subrtova, V.; Petricek, V.; Maly, K. *Collect. Czech. Chem. Commun.* **1991**, *56*, 1983.
- (18) The symmetry operator for F1 is [-x, -1/2+y, 2-z] and [1-x, -1/2+y, 2-z] respectively.
- (19) ESTRON10, Busetta, B.; Courseille, C.; Hospital, M. *Acta Crystallogr. B*, **1973**, *29*, 298.
- (20) Symmetry operators are [-x, -1/2+y, -z], [1-x, -1/2+y, 1-z] and [1+x, y, z] respectively.
- (21) Bruker (2010). *APEX2 v2010.7-0*. Bruker AXS Inc., Madison, Wisconsin, USA.

TOC

